Name: Bohui Jia; Student ID: 2842971.

Chapter 1 Comm System with AWGN

1.1 Introduction: "Additive White Gaussian Noise", or AWGN, has been chosen as an ideal approach to approximate the noises in the communication systems. As it has a particular character of independent observations at different times (specifically described in Appendix 1). Gaussian noise interferes with the received signal. The amplitude and phase of the Gaussian noise vary randomly, causing changes in the amplitude and phase of the received signal. This makes the signal analysis and decoding more challenging. The presence of Gaussian noise blurs the signal during transmission, thereby reducing its quality and reliability.

The Low-pass Nyquist Filter is introduced to solve Inter-Symbol Interference (ISI) brought by AWGN. According to Nyquist's First Criterion, to avoid inter-symbol interference (ISI), at each symbol timing point ($\mathrm{t} = \mathrm{nT}$, where T is the symbol period), the filter's response should reach a peak, while the response at other sampling points should be zero. A traditional implement of the Low-pass Nyquist Filter is the raised cosine filter, mathematically represented in the frequency domain as:

$$H_{rc}(f) = \begin{cases} 1, |f| \le \dfrac{1-\beta}{2T_s} \\ \dfrac{1}{2}\left[1+\cos\left(\dfrac{\pi T_s}{\beta}\right)[|f| - \dfrac{1-\beta}{2T_s}]\right], \dfrac{1-\beta}{2T_s} < |f| \le \dfrac{1+\beta}{2T_s} \\ 0, otherwise \end{cases} \tag{1}$$

Where β is the roll-off factor; T_s is the symbol time.

1.2 Methodology: In this section, I choose the square-root-raised-cosine filter, SRRC to minimize the ISI. The SRRC's frequency response is the square root of that of RC, which is:

$$\begin{gathered} H_{rc}(f) = H_{rrc}(f) \cdot H_{rrc}(f) \\ |H_{rrc}(f)| = \sqrt{(|H_{rc}(f)|)} \end{gathered} \tag{2}$$

Where, $H_{rc}(f)$ is the frequency response of RC; $H_{rrc}(f)$ is the frequency response of SRRC. The unit impulse response of $H_{rc}(f)$ could derived by applying inverse Fourier transform to $H_{rrc}(f)$, which is:

$$h(t) = \begin{cases} \dfrac{1}{t_s}\left(1+\beta\left(\dfrac{4}{\pi}-1\right)\right), \quad t=0 \\ \dfrac{\beta}{T_s\sqrt{(2)}}\left[\left(1+\dfrac{2}{\pi}\right)sin\left(\dfrac{\pi}{4\beta}\right)+\left(1-\dfrac{2}{\pi}\right)cos\left(\dfrac{\pi}{4\beta}\right)\right], t = \pm\dfrac{T_s}{4\beta} \\ \dfrac{1}{T_s}\dfrac{sin\left[\pi\dfrac{t}{T_s}(1-\beta)\right]+4\beta\dfrac{t}{T_s}cos\left(\dfrac{t}{T_s}(1+\beta)\right)}{\pi\dfrac{t}{T_s}\left[1-\left(4\beta\dfrac{t}{T_s}\right)^2\right]}, otherwise \end{cases} \tag{3}$$

Where β is the roll-off factor of the SRRC.

To study the effort of β and design a suitable filter for that task, I implemented a SRRC using "rcosdesign" (set the type to 'sqrt') to draw the response of SRRCs under different settings of β.

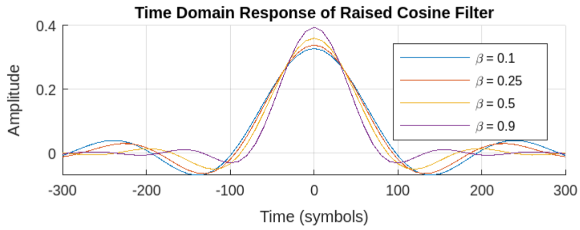

Figure 1(a) Time Domain Response of SRRC

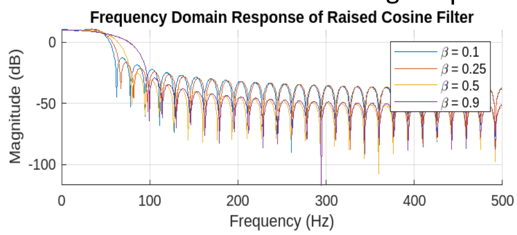

Figure 1(b) Frequency Domain Response of SRRC

In figure 1(a), we can see that: while roll-off factor decreases, the tailing effort pronounced more, which means a higher requirement on bit timing accuracy but a lower bandwidth

utilization ($\eta = \frac{2f_N}{(1+\beta)f_N} = \frac{2}{1+\beta}$, *where f_N is the nyquist bandwidth*). In practical usage, to balance the bandwidth occupation and tailing effort, the β is typically chosen from $0.25\sim0.5$.[1]
To evaluate the performance of the SRRC filters, I made a comparation with the theoretical values in the upcoming sections, which comes from:

$$BER = \frac{4}{\log_2(M)}\left(1-\frac{1}{\sqrt{M}}\right)Q\left(\sqrt{\frac{3\log_2(M)}{M-1}\cdot\frac{E_b}{N_0}}\right), M = 64 \tag{4}$$

Using Shannon Channel Capacity Formula, the minimum value of E_b/N_0 can be derived as:

$$C = Blog_2(1+E_b/N_0), E_b/N_0 \geq 2^{\frac{5}{4}} - 1$$
$$E_b/N_0 \ \geq \ 1.398\text{db} \tag{5}$$

1.3 Results and Discussion: For that section, to study the effort of SRRC's parameters, I will:

1.3.1 Analyse the effort of β by plotting the BER curve under noise SNR of 4db,6db, 8db using different roll-off factors from 0 *to* 1 with steps of 0.05.

To study the effort of the roll-off factor, I limited beta to be the only variable for this experiment. The following system parameters are controlled, as shown in Table 1. The result of this part is shown in Figure 2.

QAM Size (Alphabet size)	64
Filter Span	8
Oversampling rate	10
Symbol Amount	1000

Table 1 Parameters of the system.

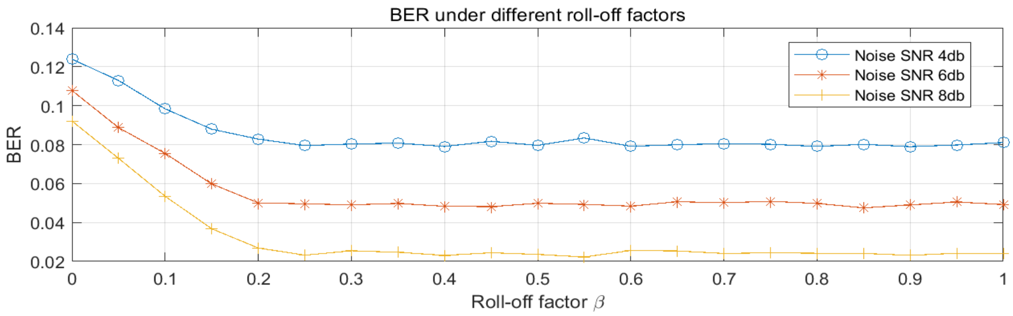

Figure 2 BER with Gaussian Noise

As shown in Figure 2, the BER curve of 4db and 8db noise SNR saw a dramatic decrease in $\beta \in [0,0.2]$, then bottomed at $\beta \approx 0.25$ and fluctuated around 0.08 and 0.025 until β reached 1; Similarly, the curve of 6db shows a drop when $\beta \in [0,0.2]$ and a slight oscillation around 0.05. However, it reached the minimal value at $\beta \approx 0.3$.
From the experiment, we can derive that: A higher roll-off factor can reduce the ISI better. However, it will also cost more bandwidth which indicates a worse usage. To balance the bandwidth consumption while keeping ISI at an acceptable margin, I will set β to 0.3 in the following sections.

1.3.2 Plot the BER curve using span of [2,4,6,8,10] with noise SNR from 2db to 20db, step by 2db

Apart from the roll-off factor, the filter span is another important parameter of the SRRC. To study the effort of this parameter, I designed an experiment that modifies the span of filters while keeping other parameters controlled as Table 2, and the result is shown in Figure 3.

QAM Size (Alphabet size)	64
Roll-off factor	0.3
Oversampling rate	10
Symbol Amount	10000

Table 2 Parameters of the system.

[1] Tranter, William H., K. Sam Shanmugan, Theodore S. Rappaport, and Kurt L. Kosbar. Principles of Communication Systems Simulation with Wireless Applications. Upper Saddle River, NJ: Prentice Hall, 2004.

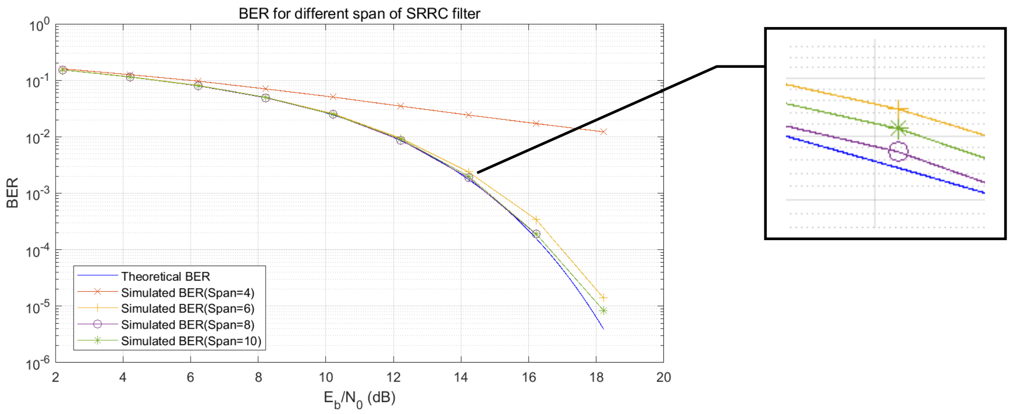

Figure 3 BER with Gaussian Noise

Figure 3 demonstrates the variation of BER using different spans for SRRC filters. The test results have a dramatic difference with the theoretical curve when noise SNR (E_b/N_0) raises. Though other curves align theoretical curve well when $E_b/N_0 \in [2db, 12db]$, there is a noticeable deviation for the curve when span equals to 4, 6 or 8 in a higher E_b/N_0, however, through all settings, the setting of span=10 performs best, which has a minimal deviation with the theoretical curve, which makes me set span to 10 in the following section.

1.3.3 Simulate a comm system with SRRC ($\boldsymbol{\beta = 0.3, \text{span} = 10}$).

The system's structure is shown in Figure 4, and the simulation results are shown in Figure 5.

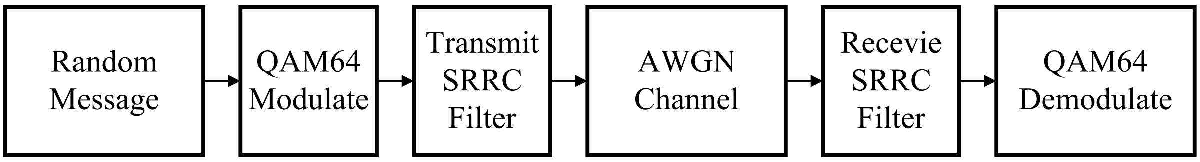

Figure 4 Simulation Structure

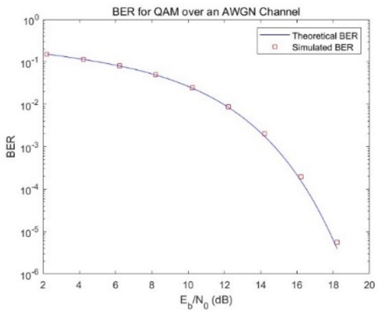

Figure 5(a) BER Curve

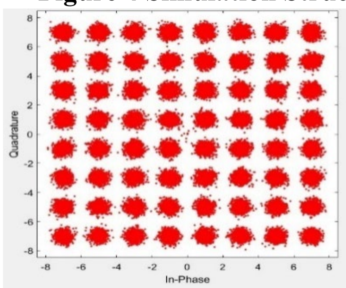

Figure 5(b) Constellation Plot for $E_b/N_0 = 16db$

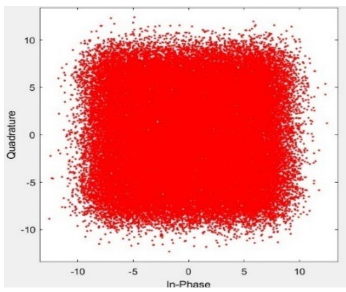

Figure 5(c) Constellation Plot for $E_b/N_0 = 2db$

As shown in Figure 5(a), with the noise SNR increasing, the BER saw a trend of reduction. Compared with the theoretical BER curve, the simulation result has a tiny difference in lower noise ($\frac{E_b}{N_0} \geq 14db$) but it fits the theoretical curve well in most areas, indicating a good performance in reducing ISI.

1.4 Conclusion: This chapter describes the character of the SRRC filters, as well as why it is important to communication systems. Then, I designed a series of experiments to find suitable parameters for the QAM64 system. The result of 1.3.3 shows that, the SRRC filters can noticeably increase the robustness of communication links, indicating the effectiveness of chosen parameters.

1.5 Appendix 1: Why choose the AWGN to model the noises in communication systems? According to the Wiener-Khinchin Theorem, the power spectral density and autocorrelation function of a random signal form a pair of Fourier transforms. Since the power spectral density of the white noise is a constant, its autocorrelation function is a Dirac delta function, indicating the observations of different times have no correlation. For the Gaussian noise, two Gaussian random variables are independent when they are uncorrelated, aligning the objective reality of the noise's observations is independent.

Chapter 2 Phase Noise and Phase Offset.

2.1 Introduction: Communication links, such as those used in wired, wireless, or optical systems, are susceptible to impairments that degrade the quality of transmitted signals. These impairments can affect signal integrity, reduce data rates, and cause transmission errors. Two typical impairments are phase offset and phase noise.

Phase Offset is deviations in the expected phase relationship between transmitted and received signals. This might be introduced by phase noise, multipath propagation, and hardware implementation. In the constellation plots, the phase offset can be recognised as a shift or rotation of points. This poses a threat of increasing ISI and BER by making distortions of signals.

Phase Noise is random, short-term fluctuations in the phase of a signal, typically caused by imperfections in oscillators or signal generation systems. These fluctuations result in the broadening of a signal's spectrum around its carrier frequency and can significantly impact the performance of communication and radar systems.

2.2 Methodology: To solve this problem, the unipolar baker code and phase-locked loops (fig. 6a) are introduced to this system. The preamble aids in synchronization because of Barker codes' excellent autocorrelation properties, and the PLLs will firstly compare the input signal F_{ref} with local output F_{out}, and output the error signal to Voltage-Controlled Oscillator (VCO) through the loop filter. When this closed-loop controller converges, the phase shift $\Delta\theta_{PLL}$ will approach the frequency offset, by using which can we fix the frequency offset from the transmission.

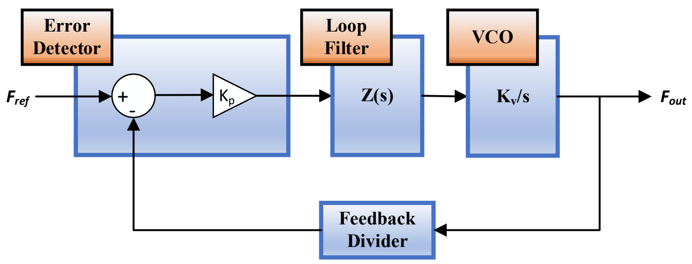

Figure 6(a) A Phase-Locked Loop

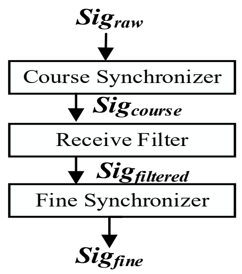

Figure 6(b) synchronizers

2.3 Results and Discussion: In this section, I designed a two-stage synchronizer as shown in Figure 6b, the course synchronizer will fix the noticeable phase shift, and the fine-sync will fix the small phase shift one more time after the receive filter. To study the effort of phase noise/offset and synchronizers, I will compare the constellation plot before/after phase noise (50dBc/Hz level and 20 Hz Freq. offset) and phase offset with E_b/N_0 set to 8db, as well as before and after synchronizations. The test results are shown in Fig. 7.

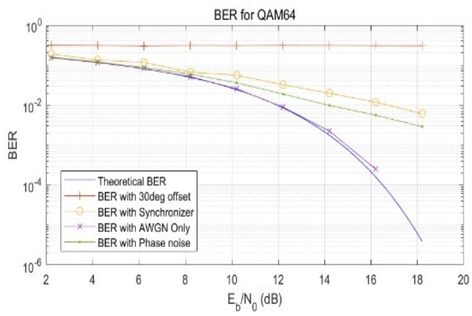

Fig. 7(a) Effort of phase noise/offset

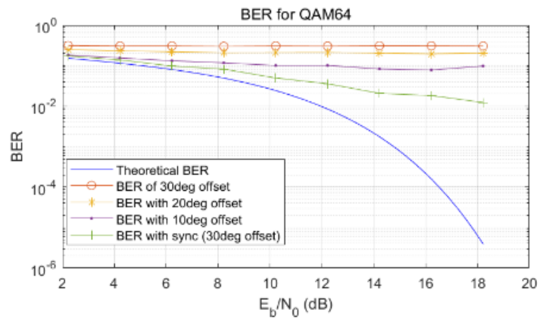

Fig. 7(b) BER with phase offsets.

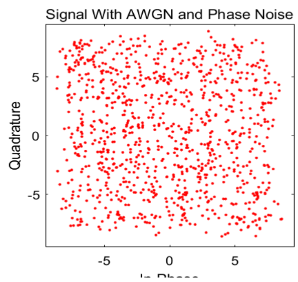

Fig. 7(c) BER with phase Noise and AWGN.

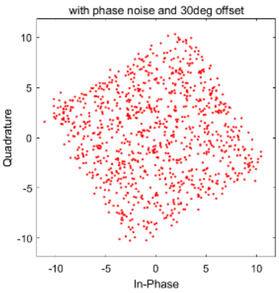

Fig. 7(d) 30deg offset

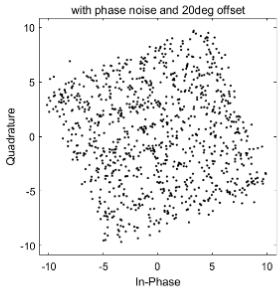

Fig. 7(e) 20deg offset

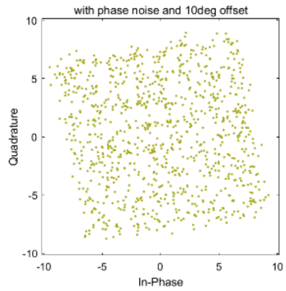

Fig. 7(f) 10deg offset

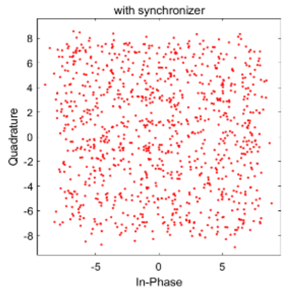

Fig. 7(g) 30deg sync.

There is more diffusion with phase noise applied (fig. 7c), leading to a higher BER than AWGN only (Fig. 7a), and more rotation as phase offset increases (Fig. 7d-7f), resulting in a higher BER (Fig. 7b) and unusable signal quality. However, when enabling PLLs (Fig. 7f), the BER saw a noticeable reduction (Fig.7a). Though there still exist deviations when $E_b/N_0 \geq 12db$, it aligns the theoretical curve well in most areas, indicating the effectiveness of synchronizers.

2.4 Conclusion: From the parts above-mentioned, the frequency noise and offsets can introduce great distortion to signals, which may influence signal quality dramatically, and the PLL-based synchronizers have notable improvement in solving the frequency offset.

Chapter 3 Comm System with Fast Fading Channels and Two-Ray Channel

3.1 Introduction:

Fast fading is a rapid variation in the amplitude, phase, or frequency of a communication signal caused by multipath propagation. It occurs when a transmitted signal reaches the receiver through multiple paths due to reflection, diffraction, and scattering from environmental obstacles. Two classic models of fast fading are Rician and Rayleigh channel.

Rician channel includes a line-of-sight (LOS) path along with multiple non-LOS paths (multipath). The received signal is the superposition of the LOS and multipath components. This model is suitable for open areas or environments with a clear LOS.

Rayleigh Channel has no significant LOS path, the signal reaches the receiver only through reflections, scattering, and diffraction (multipath propagation). The received signal strength follows a Rayleigh distribution, resulting in more severe fading. This model is suitable for urban or indoor environments with complex propagation conditions.

Two-Ray model is a simplified propagation model that accounts for the direct path and a single reflected path between a transmitter and receiver. This model is particularly useful for scenarios with flat terrain or large reflecting surfaces. Mathematically, two-ray model for discrete signal can be expressed as:

$$r[n] = \frac{\sqrt{P_t} \cdot G_t \cdot G_r \cdot \lambda}{4\pi d} \cdot s[n] + \Gamma \cdot \frac{\sqrt{P_t} \cdot G_t \cdot G_r \cdot \lambda}{4\pi d'} \cdot s[n-\tau] \tag{6}$$

Where $r[n]$ is the received signal and $s[n]$ is the transmitted signal; P_t is transmitted power; $G_t \cdot G_r$ is gains of transmitter and receiver, respectively; λ is the wavelength of the signal; d and d' are the distance of the LOS path and reflected path, respectively; τ is the delay caused by the reflected path, specifically:

$$\tau = \frac{(d' - d)}{c \cdot T_s} \tag{7}$$

Where c is the speed of light, and T_s is the sampling period.

3.2 Methodology: In this section, I implemented the two-ray model, the Rayleigh channel and the Rician channel by using dsp.delay, comm.rayleighchannel, comm.ricianchannel. To solve the problems brought by the above-mentioned fading models, I implemented a Multi-Input-Multi-

Output (MIMO) system to increase the robustness of the transmission. In the MIMO system, there are 4 transmission antennas with 4 for receiving, and to improve the signal quality, the OSTBC (Orthogonal Space-Time Block Code) is introduced. It encodes data across spatial and temporal dimensions while maintaining low decoding complexity.

3.3 Results and Discussion: To study the effort of 2-ray interference and fast-fading models, I will compare the BER curve of the above-mentioned 2-ray channel, a Rayleigh channel consisting of 2 paths (parameters shown as Tab.3a) and a Rician channel (0db gain and 0ms delay for the LOS, and a scattered path with 3ms delay and -10db gain). For the MIMO solution, I designed a 4x4 MIMO system and tested it with the same Rician fading model to make a comparison. Test results are shown in Fig. 8.

Path No.	Path Delay (ms)	Path Gain (db)	Doppler Spectrum	Max Doppler Shift
1	0	2	Gaussian, 0.6	30Hz
2	0.15	3	Flat	

Table 3 Parameters for Rayleigh Channel

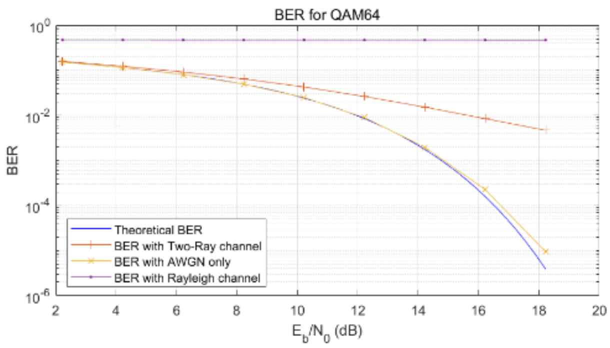

Fig. 8a BER of Rayleigh and Two-Ray channel

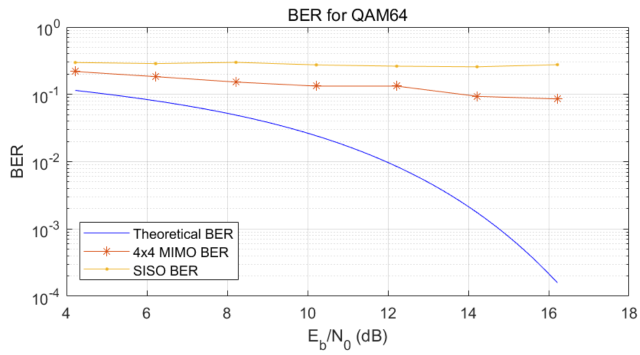

Fig. 8b BER for MIMO/SISO over Rician channel.

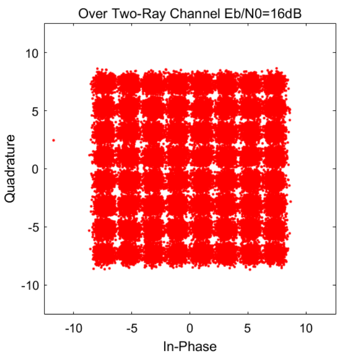

Fig.8c with Two-Ray model

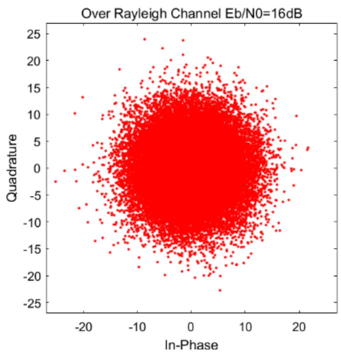

Fig. 8d with Rayleigh model

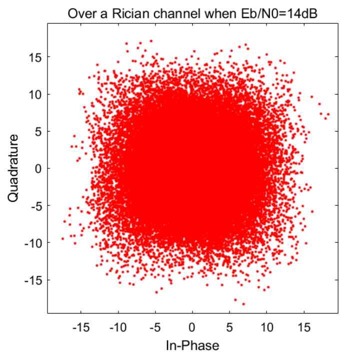

Fig. 8e with Rician model

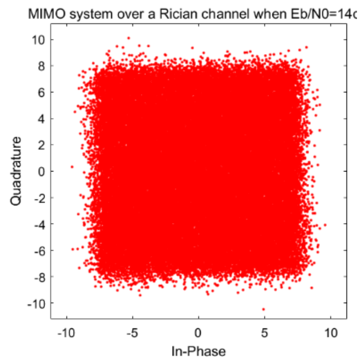

Fig. 8f with 4x4 MIMO

Fig. 8a demonstrates the effort of the two-ray and Rayleigh channel. When the Two-Ray model was applied, the BER saw an increase, indicating the interference brought by the reflected signal (fig. 8c). However, the influence of the Rayleigh channel was even more massive (fig.8d), which almost damaged the signal quality. The Rician channel has a similar impact on signal (fig. 8e), resulting in bad signal quality and a high BER (fig. 8b). According to Fig.8b, the MIMO system is verified for improving signal quality over fast-fading channels, though the BER curve still has a noticeable deviation from the theoretical one, it halved BER comparing with traditional SISO system, indicating the effectiveness of this solution.

3.4 Conclusion

In this section, I studied the effort of Two-Ray channel and 2 classic fast-fading channels and proposed a MIMO system equipped with OSCTBC. These channels resulted in a massive influence on signal quality, which posed an obstacle to communication systems, and the MIMO system was verified to be a potential solution for that sort of problem.